DOI: 10.1002/chem.201001626

# Tetra- to Dodecanuclear Oxomolybdate Complexes with Functionalized Bisphosphonate Ligands: Activity in Killing Tumor Cells

**Jean-Daniel Compain,[a] Pierre Mialane,[a] Jérôme Marrot,[a] Francis Sécheresse,[a] Wei Zhu,[b] Eric Oldfield,*[b, c] and Anne Dolbecq*[a]**

**Abstract:** We report the synthesis and characterization of five novel Mo-containing polyoxometalate (POM) bisphosphonate complexes with nuclearities ranging from 4 to 12 and with fully reduced, fully oxidized, or mixed-valent ($Mo^V$, $Mo^{VI}$) molybdenum, in which the bisphosphonates bind to the POM cluster through their two phosphonate groups and a deprotonated 1-OH group. The compounds were synthesized in water by treating $[Mo^V_2O_4(H_2O)_6]^{2+}$ or $[Mo^{VI}O_4]^{2-}$ with $H_2O_3PC(C_3H_6NH_2)OPO_3H_2$ (alendronic acid) or its aminophenol derivative, and were characterized by single-crystal X-ray diffraction and $^{31}P$ NMR spectroscopy. $(NH_4)_6[(Mo^V_2O_4)(Mo^{VI}_2O_6)_2(O_3PC(C_3H_6NH_3)OPO_3)_2]\cdot 12H_2O$ (**1**) is an insoluble mixed-valent species. $[(C_2H_5)_2NH_2]_4[Mo^V_4O_8(O_3PC(C_3H_6NH_3)OPO_3)_2]\cdot 6H_2O$ (**2**) and $[(C_2H_5)_2NH_2]_6[Mo^V_4O_8(O_3PC(C_{10}H_{14}NO)OPO_3)_2]\cdot 18H_2O$ (**4**) contain similar tetranuclear reduced frameworks. $Li_8[(Mo^V_2O_4(H_2O))_4(O_3PC(C_3H_6NH_3)OPO_3)_4]\cdot 45H_2O$ (**3**) and $Na_2Rb_6[(Mo^{VI}_3O_8)_4(O_3PC(C_3H_6NH_3)OPO_3)_4]\cdot 26H_2O$ (**5**) are alkali metal salts of fully reduced octanuclear and fully oxidized dodecanuclear POMs, respectively. The activities of **2**–**5** (which are water-soluble) against three human tumor cell lines were investigated in vitro. Although **2**–**4** have weak but measurable activity, **5** has $IC_{50}$ values of about 10 μM, which is about four times the activity of the parent alendronate molecule on a per-alendronate basis, which opens up the possibility of developing novel drug leads based on Mo bisphosphonate clusters.

**Keywords:** antitumor agents · bisphosphonates · molybdenum · O ligands · polyoxometalates

## Introduction

Bisphosphonates, such as alendronate (Fosamax), risedronate (Actonel), ibandronate (Boniva) and zoledronate (Zometa), are important drugs used to treat osteoporosis, Paget's disease, and hypercalcemia due to malignancy.[1] In addition, they have been found to kill tumor cells[2] and activate γδ T cells (containing the Vγ2Vδ2 T cell receptor) to kill tumor cells, and zoledronate has been found to switch tumor-associated macrophages from an M2 (tumor-promoting) phenotype to an M1 (tumor-killing) phenotype.[3] Furthermore, they are active in killing a broad range of protozoan parasites both in vitro[4] and in vivo,[5] and are thus of interest as both anticancer and anti-infective agents. All commercially available bisphosphonate drugs are geminal bisphosphonates and have a common P-C-P backbone (Scheme 1a) together with an $R^1$ hydroxyl group that increases the affinity of bisphosphonates for bone mineral and is known as the "bone hook". The $R^2$ group determines the potency of the bisphosphonates, all of which function by inhibiting the enzyme farnesyl diphosphate synthase in osteoclasts.[1] Alendronate ($R^1=OH$, $R^2=CH_2CH_2CH_2NH_2$) is one of the most popular bisphosphonates and has been sold for many years as a treatment for osteoporosis. Bisphosphonates are also known to be good metal-complexing agents,

[a] J.-D. Compain, Prof. P. Mialane, Dr. J. Marrot, Prof. F. Sécheresse, Dr. A. Dolbecq
Institut Lavoisier de Versailles, UMR CNRS 8180
Université de Versailles Saint Quentin
78035 Versailles cedex (France)
Fax: (+33) 1-39254381
E-mail: dolbecq@chimie.uvsq.fr

[b] W. Zhu, Prof. Dr. Dr. E. Oldfield
Center for Biophysics and Computational Biology
607 South Mathews Avenue, Urbana, Illinois 61801 (USA)

[c] Prof. Dr. Dr. E. Oldfield
Department of Chemistry
University of Illinois at Urbana-Champaign
600 South Mathews Avenue, Urbana, Illinois 61801 (USA)
Fax: (+1) 217-244-0997
E-mail: eo@chad.scs.uiuc.edu

Supporting information for this article is available on the WWW under http://dx.doi.org/10.1002/chem.201001626.

  

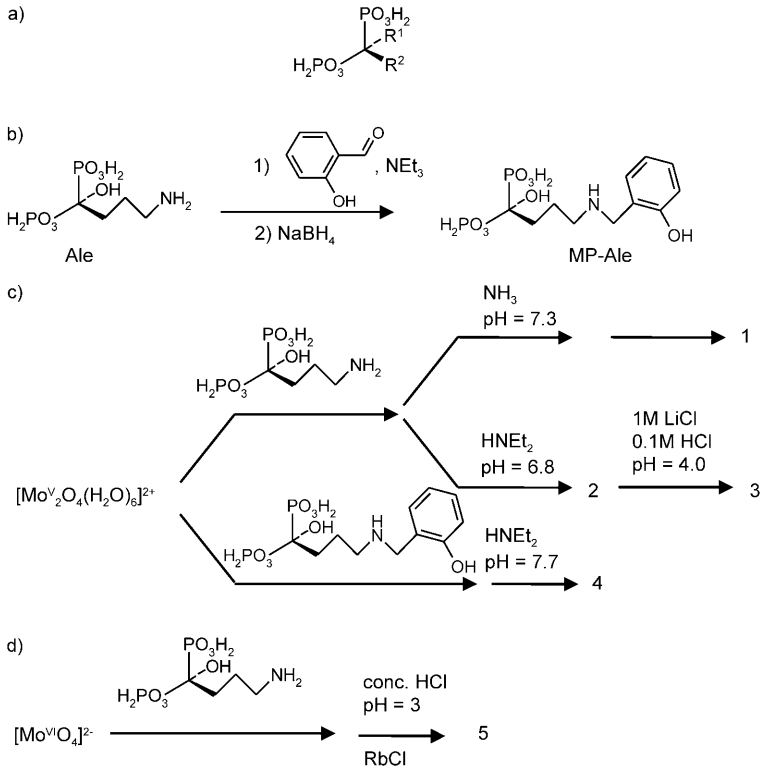


Scheme 1. a) General formula of the geminal bisphosphonates used for medical applications. b) Reaction scheme for the synthesis of bisphosphonate ligand $H_4O_3PC(C_{10}H_{14}NO)(OH)PO_3$ (**MP-Ale**). c, d) Synthetic pathways for polyoxometalates **1**–**5**.

and many bisphosphonate compounds, which vary from molecular complexes to three-dimensional coordination frameworks, have been structurally characterized.[6] Among these complexes, polyoxometalates (POMs) are of interest because POMs themselves have interesting medicinal properties, including antitumor and antiretroviral activity,[7] and POM hybrid clusters lead to selective cell adhesion to surfaces.[8]

Polyoxometalates are often considered to be soluble molecular oxides. They are built by connecting $\{MO_x\}$ polyhedra, in which M is a d-block element in a high oxidation state, usually $V^{IV,V}$, $Mo^{VI}$, or $W^{VI}$.[9] Earlier, Sergienko et al. reported the crystallographic structures of the reaction products of $Mo^{VI}$ and $W^{VI}$ ions with bisphosphonates, mainly etidronate.[10] In parallel, Kortz and Pope isolated the polymeric $W^{VI}$ derivative $\{[(O_3PCHN(CH_3)_2PO_3)W_2O_6]^{4-}\}_\infty$,[11] as well as the hexanuclear $Mo^{VI}$ POM, $[(O_3PCH_2PO_3)Mo_6O_{18}(H_2O)_4]^{4-}$.[12] More recently, Wang et al. described the synthesis of two mixed $V^{IV}/Mo^{VI}$ species, one with etidronate, the other with alendronate.[13] We initiated a study of the reactivity of the reduced dinuclear $\{Mo^V_2O_4\}^{2+}$ group with bisphosphonates, starting with the simplest species, methylenediphosphonate ($R^1=H$, $R^2=H$), and reported a large family of ring-shaped reduced POMs built up by alternating organic ligands and dimers of edge-sharing $Mo^V$ octahedra with the general formula $\{(Mo^V_2O_4)(O_3PCH_2PO_3)\}_n$ ($n=3$, 4, 6, 10).[14] Some of these compounds encapsulated extra ligands, such as carbonate,[14a] sulfite,[14b] or methylarsenate.[14c] These anions have been successfully used as both reductants and as stabilizing agents for the synthesis of metallic nanoparticles ($Pd^0$, $Pt^0$, $Ag^0$),[14c,15] and we recently extended this family of compounds by using the commercial drug etidronate ($R^1=OH$, $R^2=CH_3$).[16]

Of the POMs isolated so far with etidronate, only the one with a cyclohexane-like shape is analogous to those obtained with methylenediphosphonate. The other species that have been isolated are the tetranuclear anion $[(Mo^V_2O_4)(O_3PC(CH_3)O)PO_3)_2]^{6-}$ and the tetradecanuclear ring $[(Mo^V_2O_4)_7(O_3PC(CH_3)(OH)PO_3)_2(CH_3COO)_7]^{21-}$. To date, no POMs with bisphosphonate ligands have been studied for activity in cells. We thus decided to explore the reactivity of $Mo^V$ and $Mo^{VI}$ ions with more complex bisphosphonates that, on their own, have tumor-cell-killing activity, starting with the commercially used drug alendronate ($R^1=OH$, $R^2=(CH_2)_3NH_2$),[17] with the aim being to see if more potent activity could be obtained. Herein we describe the synthesis and crystallographic and $^{31}P$ NMR spectroscopic characterization of four novel POMs containing alendronate (**Ale**): two with $Mo^V$, one with $Mo^{VI}$, and an insoluble mixed-valent POM. We also report the synthesis of an aminophenol derivative (**MP-Ale**) of the alendronate ligand with enhanced binding capacity to transition-metal ions, and a tetranuclear $Mo^V$ compound that incorporates this new ligand. Compounds were then screened for tumor-cell-killing ability in vitro.

## Results and Discussion

**Crystal structures**: In the five crystal structures determined, the 1-hydroxyl group of the bisphosphonate ligand is found to be deprotonated and coordinates to either one or two metal ions (Scheme 2). Valence bond calculations[18] (Figures SI1–SI5 in the Supporting Information) support the proposed oxidation states of Mo in **1**–**5** and the deprotonation of the hydroxyl groups, and also indicate the presence of terminal water molecules in **3**. The anion in **1** (Figure 1a) is built up by connecting three dimeric units, one of which contains two edge-sharing $Mo^V$ octahedra and the others are

  

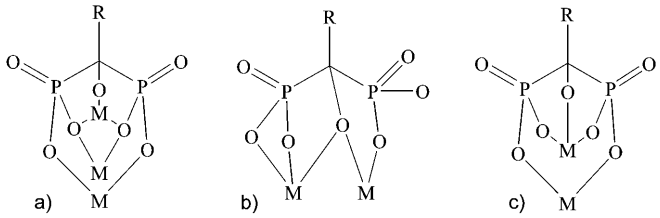


Scheme 2. Coordination modes of the bisphosphonate ligands in a) complexes **1** and **5**, b) complexes **2** and **4**, and c) complex **3**.

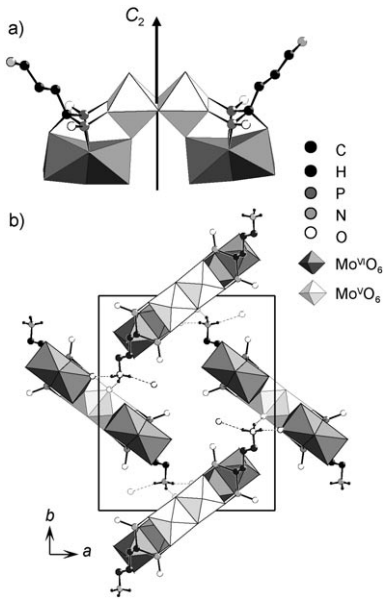


Figure 1. a) Mixed ball-and-stick and polyhedral representation of the mixed-valent anion $[(Mo^{V}_2O_4)(Mo^{VI}_2O_8)_2(O_3PC(C_3H_6NH_3)OPO_3)_2]^{6-}$ in **1**. The arrow indicates the position of the symmetry axis. b) 3D structure of **1** with intermolecular hydrogen bonds. Some H atoms have been omitted for clarity.

two face-sharing $Mo^{VI}$ octahedra. Each $Mo^{V}$ octahedron shares one vertex with one $Mo^{VI}$ octahedron of each $Mo^{VI}$ dimer. The $\{PO_3\}$ groups of the bisphosphonate ligands are equivalent and connect two $Mo^{VI}$ ions and a $Mo^{V}$ ion, as illustrated in Scheme 2a. The deprotonated hydroxyl group of **Ale** binds to one $Mo^{VI}$ ion. The six Mo ions are coplanar, but the organic ligands are not located in this plane and the anion in **1** contains only one symmetry element, namely, a $C_2$ axis passing through the center of the $Mo^{V}$–$Mo^{V}$ bond (Figure 1a). The $NH_3^+$ groups of the organic ligand are involved in hydrogen bonds with a water molecule and with oxygen atoms of neighboring POMs (Figure 1b).

The anions in **2** and **4** have the same compact $Mo^{V}$ framework (Figures 2a, and 3a), similar to the structure of the tetranuclear anion $[(Mo^{V}_2O_4)(O_3PC(CH_3)O)PO_3)_2]^{6-}$, except that the etidronate ligands are replaced by **Ale** or **MP-Ale** ligands in **2** and **4**, respectively. They contain a centrosymmetric rhomboid $\{Mo^{V}_4O_{16}\}$ core, which is commonly encountered in $Mo^{V}$ chemistry.[19]

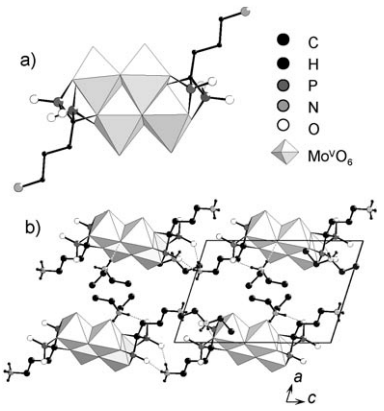


Figure 2. a) Mixed ball-and-stick and polyhedral representation of the fully reduced tetranuclear anion $[Mo^{V}_4O_8(O_3PC(C_3H_6NH_3)OPO_3)_2]^{4-}$ in **2**. b) 3D structure of **2** with intermolecular hydrogen-bonding interactions. Some H atoms have been omitted for clarity.

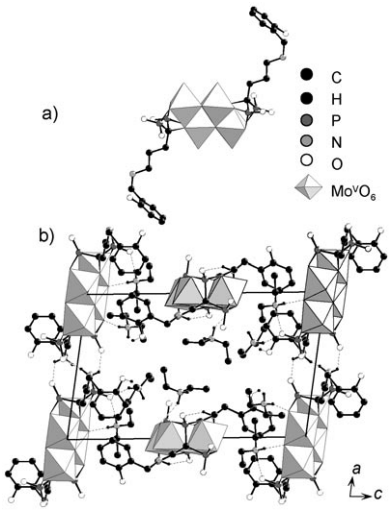


Figure 3. a) Mixed ball-and-stick and polyhedral representation of the fully reduced tetranuclear anion $[Mo^{V}_4O_8(O_3PC(C_{10}H_{14}NO)OPO_3)_2]^{6-}$ in **4**. b) 3D structure of **4** with intermolecular hydrogen-bonding interactions. Some H atoms have been omitted for clarity.

The crystallographically equivalent bisphosphonate ligands act as tetradentate ligands (Scheme 2b) and connect dissymmetrically to the Mo ions. Indeed, one $\{PO_3\}$ group is mono-coordinated to a $Mo^{V}$ center, whereas the other phosphonato group is coordinated via two oxygen atoms to an adjacent metallic center. Additionally, the deprotonated hydroxyl group acts as a $\mu_2$-O ligand. In both structures, the counterions are dimethylammonium cations, which establish hydrogen bonds with the POMs (Figures 2b and 3b). However, these two compounds are not isostructural and their three-dimensional structures are also different. Indeed, the Mo frameworks of the POMs in **2** are parallel, whereas in **4** they are perpendicular, probably because the ligand in **4** is far bulkier than that in **2**.

The structure of the octanuclear anion in **3** (Figure 4a) has not been observed previously in this family of $Mo^{V}$

  

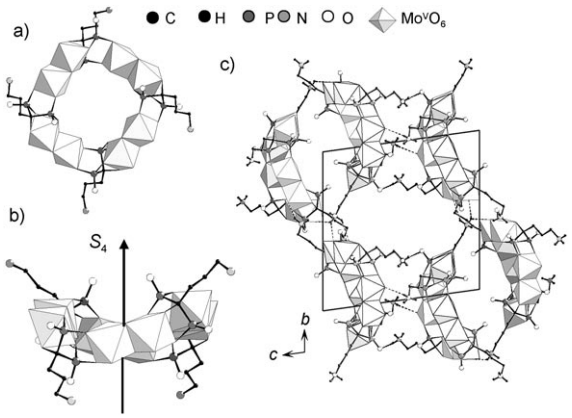


Figure 4. a, b) Mixed ball-and-stick and polyhedral representations of the paddle-wheel-shaped $[(Mo^{V}_2O_4(H_2O))_4(O_3PC(C_3H_6NH_3)OPO_3)_4]^{8-}$ anion in **3** in two different orientations. The arrow indicates the position of the pseudosymmetry axis. c) 3D structure of **3** with intermolecular hydrogen-bonding interactions. Some H atoms have been omitted for clarity.

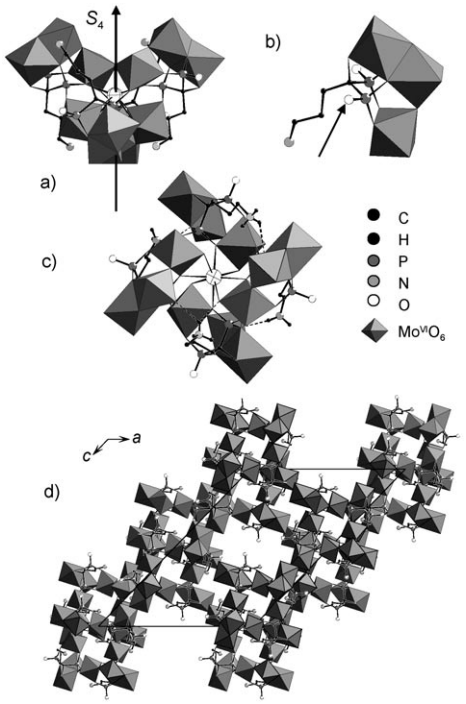


Figure 5. Mixed ball-and-stick and polyhedral representation of a) the $Mo^{VI}$ anion $[(Mo^{VI}_3O_8)_4(O_3PC(C_3H_6NH_3)OPO_3)_4]^{8-}$ in **5** (the arrow indicates the position of the symmetry axis and runs through the central octa-coordinated Na ion) and b) the trimeric building unit in **5** (the arrow indicates the position of the oxygen atom of the P=O group involved in a P-O-Mo bond with an adjacent trimeric unit). c) Representation of the anion in **5** showing the intramolecular hydrogen bonds. d) 3D structure of **5**. Some H atoms have been omitted for clarity.

bisphosphonate complexes. It is built up from four $Mo^{V}$ dimers that do not share any oxygen atoms and are only linked by **Ale** molecules acting as pentadentate ligands (Scheme 2c). One of the $Mo^{V}$ ions is bound to three oxygen atoms of the organic ligand, whereas the other is only bound to two oxygen atoms of **Ale** and is also connected to a terminal water molecule. The positions of the $CH_2CH_2CH_2NH_3^+$ arms of the organic ligand around the circular Mo framework evoke a paddle-wheel shape. The Mo ions are not coplanar, however, and the wheel is twisted. There are no crystallographic symmetry elements in the structure of **3**. However, the anion has a pseudo-$S_4$ axis passing through the center of the POM framework (Figure 4b), and in the three-dimensional structure of **3**, the anions assemble in centrosymmetric structures and interact through N–H···O hydrogen bonds (Figure 4c).

The structure of the anion in **5** (Figure 5a) can be best described as an assembly of four trimeric units. A trimeric unit is built of a dimer of face-sharing $Mo^{VI}$ octahedra that has a common vertex with a monomeric $Mo^{VI}$ octahedron (Figure 5b). The **Ale** ligand acts as a hexadentate ligand with a coordination mode similar to that encountered in **1** (Scheme 2a), together with an additional connection to the monomeric $Mo^{VI}$ ion of a neighboring trimeric group through a terminal oxygen atom of one of the P=O groups (indicated by an arrow in Figure 5b). Among the six rubidium and two sodium counterions, an octacoordinate sodium ion occupies a special position at the center of the POM, acting as a template ion (as shown in Figure 5a). Intramolecular N–H···O hydrogen bonds between the amino group of the **Ale** ligand and terminal or bridging atoms of the POM core stabilize this dodecanuclear architecture (Figures 5c and SI6 in the Supporting Information), and we have recently found evidence for their key role in the intrinsic photochromic properties of these $Mo^{VI}$ species.[20] Although the anion does not lie on any crystallographic symmetry element, a pseudo-$S_4$ axis can be identified, which passes through the central sodium ion (Figure 5a), and the three-dimensional structure (Figure 5d) shows a complex network of polyoxometalate ribbons.

**$^{31}$P NMR spectroscopic characterization**: The synthetic pathways to **1**–**5** are shown in Scheme 1. We characterized these species in the solid state by single crystal X-ray diffraction (as described above) and in solution by $^{31}$P NMR spectroscopy. As described previously,[14b,21] $^{31}$P NMR spectroscopy is a powerful tool to determine whether structures characterized in the solid state are maintained in solution, for investigation of the stability of isolated compounds in solution, and for characterizing the nature of the species present in these solutions.

Compound **1** is rather insoluble in all common solvents. Nevertheless, two features can be seen: 1) the $^{31}$P NMR spectrum of a freshly prepared solution of **1** indicates the presence of the octanuclear anion $[(Mo^{V}_2O_4(H_2O))_4(O_3PC(C_3H_6NH_3)OPO_3)_4]^{8-}$, which crystallizes as **3** (Figure SI7 in the Supporting Information), and 2) the synthetic process that leads to **1** requires slow air oxidation of the reacting solution. Formation of mixed-valent species from mixtures of $[Mo_2O_4(H_2O)_6]^{2+}$ and methylenediphosphonate ligands has been previously observed and permitted isolation of the triangular anion $[(Mo^{V}_2O_4)_3(Mo^{VI}O_4)(O_3PCH_2PO_3)_3]^{8-}$, which

  

encapsulates a $\{Mo^{VI}O_4\}$ tetrahedron, and the rectangular $[(Mo^{V}_2O_4)_2(Mo^{VI}O_3)_2(O_3PCH_2PO_3)_2(HO_3PCH_2PO_3)_2]^{10-}$ species, which contains two $Mo^{VI}$ centers.[14b] The $^{31}P$ NMR spectra of freshly prepared synthetic solutions of **2** and **4** (Figure SI8 in the Supporting Information) are similar to those of crystals of **2** and **4** in water (Figure 6). These spectra exhibit a doublet of doublets, in agreement with the presence of two nonequivalent and coupled phosphorus atoms within the bisphosphonate ligand. No change is observed over a period of one week, that is, **2** and **4** are stable in pure aqueous solutions. The chemical shifts and coupling constants of **2** and **4** are very similar, and are also similar to those of the etidronate derivative $[(Mo^{V}_2O_4)_2(O_3P\{C(CH_3)O\}PO_3)_2]^{6-}$[16] (Table 1).

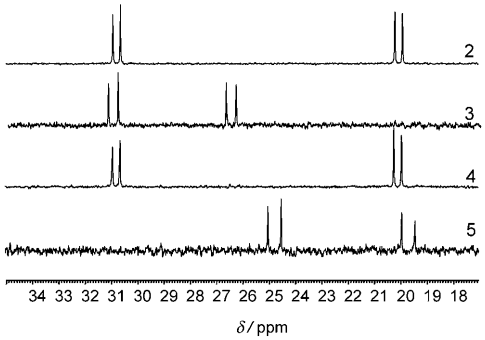


Figure 6. $^{31}P\{^1H\}$ NMR spectra of **2**–**4** dissolved in water and **5** dissolved in 1 M HOAc/NaOAc buffer.

In contrast, the $^{31}P$ NMR spectrum of **2** in the presence of $Li^+$ changes rapidly with time: a solution of **2** in 1 M LiCl (Figure 7 and SI9 in the Supporting Information) indicates degradation of **2** into three species. Slow evaporation of a solution of **2** in 1 M LiCl afforded crystals of **3**, and comparison of the $^{31}P$ NMR spectrum of **3** redissolved in water with that of a solution of **2** in 1 M LiCl permits identification of **3** as one of the three species. The other two are unknown. The $^{31}P$ NMR spectrum of **3** (Figure 6) also exhibits a doublet of doublets (as with **2** and **4**), but the splitting between the two doublets is smaller and the coupling constant is larger. As expected and similar to **2**, compound **4** degrades slowly in 1 M LiCl. Compound **5** is sparingly soluble in water but dissolves readily in 1 M NaOAc/AcOH buffer

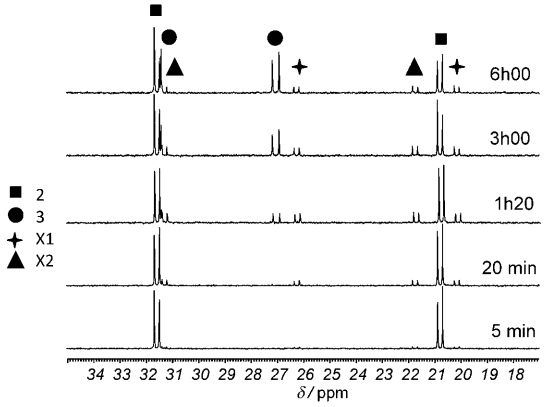


Figure 7. Evolution of the $^{31}P\{^1H\}$ NMR spectra of a solution of **2** in 1 M LiCl (pH 3.7) at RT over time; X1 and X2 are unidentified intermediate species.

Table 1. Representation of the anions and $^{31}P\{^1H\}$ NMR spectroscopic data of **2**–**5** compared with previously characterized compounds.

| | Structure | Reference | Solvent | $\delta$ [ppm] | $^2J$ [Hz] |
|---|---|---|---|---|---|
| **2** |  | this work | $H_2O$ | 30.93, 30.64, 20.19, 19.91 | 23.4 |
| **3** | 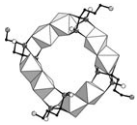 | this work | $H_2O$ | 31.17, 30.81, 26.70, 26.33 | 30.0 |
| **4** |  | this work | $H_2O$ | 30.91, 30.62, 20.20, 19.92 | 23.4 |
| **5** | 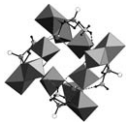 | this work | 1 M NaOAc/ HOAc | 25.02, 24.52, 19.93, 19.43 | 40.6 |
| $[(Mo^{V}_2O_4)_2(O_3PC(CH_3)O)PO_3)_2]^{6-}$ |  | [16] | $H_2O$ | 32.28, 32.10, 22.12, 21.93 | 22.1 |
| $[(Mo^{V}_2O_4)_6(OH)_6(O_3PCH_2PO_3)_6]^{18-}$ | 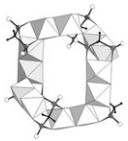 | [14c] | 1 M NaCl | 24.52, 24.40, 19.82, 19.70 | 13.7 |
| $[(Mo_2O_4)_3(O_3PCH_2PO_3)_3(CH_3AsO_3)]^{8-}$ |  | [14c] | $H_2O$ | 25.55, 25.42, 23.52, 23.39 | 15.6 |

and 1 M NaCl. As for **2–4**, the $^{31}$P NMR spectrum of **5** (Figure 6) exhibits a doublet of doublets, in accord with the presence of two nonequivalent phosphorus atoms. Moreover, solutions of **5** are stable over a period of at least one week.

**Cell-growth inhibition**: To determine whether **1–5** have activity in the inhibition of tumor-cell growth, we screened all compounds against three tumor cell lines: NCI-H460 (human nonsmall lung cancer); MCF-7 (human breast cancer), and SF-268 (human CNS cancer). Compound **1** was poorly soluble and no inhibition activity was found, but **2–5** all had measurable activity (Table 2). For compounds **2–4** the activity was worse than that of alendronate, especially on a per-alendronate basis. However, **5** was clearly more active than alendronate. Averaged over the three cell lines, alendronate had an $IC_{50}$ of about 160 μM, whereas that of **5** was about 10 μM, or about 40 μM on a per-alendronate basis, a fourfold increase in potency. Whether this enhanced activity is due to dissociation of the complex outside the cell (and uptake of alendronate and a molybdate), to dissociation inside the cell, or to POM-complex activity per se (as with, e.g., $Mo_7O_{24}^{2-}$[7c]) is unknown at this time. However, the comparison of the activity of **2–5** with that of commercial $(NH_4)_6Mo^{VI}{}_7O_{24}$ and of $LiNa[Mo^V{}_4O_8(OH)_2(H_2O)_2(C_4O_4)_2]$,[22] which do not contain any bisphosphonate ligands, suggests that the POM and the alendronate ligand have a synergic effect. In conclusion, the observation that bisphosphonate activity is enhanced is of interest, and suggests that more lipophilic bisphosphonate[2] POM complexes may have much better activity.

Table 2. Cell growth inhibition assay results for **2–5** compared to alendronate and $Mo^V$ or $Mo^{VI}$ bisphonate-free POMs.

| | NCI-H460 $IC_{50}$ [μM] | MCF-7 $IC_{50}$ [μM] | SF-268 $IC_{50}$ [μM] |
|---|---|---|---|
| **2** | 201 ± 16 | 171 ± 8 | 105 ± 32 |
| **3** | 109 ± 75 | 107 ± 21 | 365 ± 43 |
| **4** | 443 ± 67 | 126 ± 10 | 39 ± 3 |
| **5** | 12 ± 4 | 11 ± 1 | 7 ± 1 |
| Alendronate | 202 ± 43 | 126 ± 2 | 136 ± 13 |
| $LiNa[Mo^V{}_4O_8(OH)_2(H_2O)_2(C_4O_4)_2]$ | 476 ± 60 | 605 ± 1 | 457 ± 14 |
| $(NH_4)_6[Mo^{VI}{}_7O_{24}]$ | 199 ± 5 | 283 ± 29 | 183 ± 4 |

## Conclusion

Hybrid bisphosphonate POM complexes built by condensing Mo octahedra and bisphosphonate ligands with nuclearities from 4 to 12, either fully reduced, mixed-valent, or fully oxidized, have been isolated, and show the strong chelating ability of this class of ligand. As observed with previously reported Mo bisphosphonate complexes, the geometry of the POM is strongly dependent on the nature of the ligand and counterion. Although most bisphosphonate POM compounds reported in the literature are insoluble, the $Mo^{VI}$ and $Mo^V$ complexes reported here are soluble and stable in aqueous solution, with the exception of **1**, as evidenced by $^{31}$P NMR spectroscopy. Our results thus open the way to the synthesis of a large family of functionalized Mo bisphosphonates in which the nature of the organic ligand is varied. It may thus be possible to obtain hybrid POM bisphosphonates containing redox-active POMs that have potent antitumor activity and potent bisphosphonates all packed in a lipophilic complex, which would increase cell uptake and bisphosphonate potency. Further work on such systems is underway.

## Experimental Section

**Chemicals and reagents**: Alendronic acid, $H_2O_3PC(C_3H_6NH_2)(OH)PO_3H_2$ ($H_4$**Ale**), was synthesized as described in the literature.[23] All other chemicals were used as purchased without further purification. The synthetic pathways to the aminophenol derivative of **Ale** (**MP-Ale**) and to **1–5** are given in Scheme 1.

**Preparation of $[Mo_2O_4(H_2O)_6]^{2+}$ in aqueous HCl**: Hydrazine hydrate $N_2H_4{\cdot}H_2O$ (210 μL, 4.29 mmol) was added to a suspension of $MoO_3$ (2.30 g, 16.0 mmol) in aqueous HCl (4 M, 80 mL). The mixture was then stirred at 60 °C for 3 h and the resulting deep red solution (0.1 M) was allowed to cool to RT before further use.

**Synthesis of $Na_2HO_3PC(C_{10}H_{14}NO)(OH)PO_3H{\cdot}2H_2O$ [$Na_2H_2$(MP-Ale)]**: $H_4$**Ale** (5 g, 20 mmol) and salicylaldehyde (2.5 mL, 24 mmol) were dissolved in a mixture of methanol (100 mL) and triethylamine (17 mL, 120 mmol). The deep orange solution was heated to reflux for two hours, and then cooled to RT before portionwise addition of sodium borohydride (1.14 g, 30 mmol). The resulting yellow suspension was heated to reflux overnight, and then the pale yellow solid was collected by filtration under vacuum, thoroughly washed with methanol, and dried with diethyl ether (yield 73 %, 5.9 g). $^1$H NMR ($D_2O$): $\delta$ = 1.96 (m, 4H), 3.08 (t, 2H), 4.21 (s, 2H), 6.96 (m, 2H), 7.34 ppm (m, 2H); $^{31}$P NMR ($D_2O$): $\delta$ = 21.1 ppm (s); elemental analysis calcd (%) for $C_{11}H_{17}NNa_2O_8P_2$: C 30.36, H 4.86, N 3.22, Na 10.56, P 14.23; found: C 29.71, H 4.73, N 3.12, Na 9.75, P 14.29.

**Synthesis of $(NH_4)_6[(Mo^V{}_2O_4)(Mo^{VI}{}_2O_6)_2(O_3PC(C_3H_6NH_3)OPO_3)_2]{\cdot}12H_2O$ (1)**: $H_4$**Ale** (0.156 g, 0.625 mmol) was dissolved in aqueous $[Mo_2O_4(H_2O)_6]^{2+}$ (0.1 M, 6.25 mL, 0.625 mmol) synthesized as described above. Aqueous ammonium hydroxide (33 %, 1.8 mL, 15 mmol) was then added dropwise to pH 7.3. The resulting deep red solution was filtered, and then left to evaporate at RT. After 2 d, large red parallelepipedic crystals were collected by filtration (0.122 g, 37 % based on Mo). IR (KBr pellets): $\tilde{\nu}$ = 1458 (m), 1398 (s), 1268 (w), 1136 (s), 1076 (s), 1053 (vs), 1021 (s), 988 (m), 923 (s), 912 (s), 874 (vs), 816 (s), 787 (sh), 752 (w), 734 (sh), 706 (m), 668 cm$^{-1}$ (m); elemental analysis calcd (%) for $C_8H_{66}O_{44}N_8P_4Mo_6$: C 5.72, H 3.96, N 6.68, P 7.38, Mo 34.30; found: C 6.10, H 4.06, N 6.95, P 7.69, Mo 35.71.

**Synthesis of $[(C_2H_5)_2NH_2]_4[Mo^V{}_4O_8(O_3PC(C_3H_6NH_3)OPO_3)_2]{\cdot}6H_2O$ (2)**: $H_4$**Ale** (0.156 g, 0.625 mmol) was dissolved in aqueous $[Mo_2O_4(H_2O)_6]^{2+}$ (0.1 M, 6.25 mL, 0.625 mmol) prepared as described above. Diethylamine (2.8 mL, 27 mmol) was added dropwise to pH 6.8. The resulting deep red solution was filtered and left to evaporate at RT. Small, red, parallelepipedic crystals were collected by filtration the following day (0.211 g, 48 % based on Mo). $^1$H NMR ($D_2O$): $\delta$ = 1.14 (t, 24H), 1.97 (m, 4H), 2.34 (m, 2H), 2.96 ppm (q, 16H); IR (KBr pellets): $\tilde{\nu}$ = 1558 (w), 1453 (m), 1391 (w), 1165 (s), 1139 (vs), 1113 (s), 1058 (sh), 1046 (s), 1029 (s), 965 (vs), 936 (s), 891 (m), 845 (w), 811 (m), 737 cm$^{-1}$ (s); elemental analysis calcd (%) for $C_{24}H_{78}Mo_4N_6O_{28}P_4$: C 20.59, H 5.59, N 5.97, P 8.81, Mo 27.28; found: C 20.76, H 5.52, N 6.05, P 8.92, Mo 27.64;

  

**Synthesis of $Li_8[(Mo^V_2O_4(H_2O))_4(O_3PC(C_3H_6NH_3)OPO_3)_4]\cdot 45H_2O$ (3)**: Compound **2** (0.2 g, 0.14 mmol) was dissolved in aqueous LiCl (1 M, 14 mL). Aqueous hydrochloric acid (0.1 M) was added dropwise to pH 4.0. The red solution was left to evaporate at RT. Large red parallelepipedic crystals were collected by filtration after 2 d (0.142 g, 68% based on Mo). $^1$H NMR ($D_2O$): $\delta = 2.26$ (m, 4H); 3.07 ppm (t, 2H); IR (KBr pellets): $\tilde{\nu} = 1518$ (m), 1470 (w), 1451 (w), 1396 (w), 1153 (s), 1127 (s), 1065 (vs), 1029 (s), 948 (vs), 917 (sh), 745 cm$^{-1}$ (m); elemental analysis calcd (%) for $C_{16}H_{134}Li_8Mo_8N_4O_{93}P_8$: C 6.53, H 4.59, N 1.90, P 8.42, Li 1.89, Mo 26.09; found: C 6.67, H 4.09, N 1.82, P 8.68, Li 1.88, Mo 26.11.

**Synthesis of $[(C_2H_5)_2NH_2]_6[Mo^V_4O_8(O_3PC(C_{10}H_{14}NO)OPO_3)_2]\cdot 18H_2O$ (4)**: $Na_2H_2$(**MP-Ale**) (0.544 g, 1.25 mmol), synthesized as described above, was dissolved in a 0.1 M solution of $[Mo_2O_4(H_2O)_6]^{2+}$ (12.5 mL, 1.25 mmol). Diethylamine (5.4 mL, 52 mmol) was added dropwise to pH 7.7. The resulting deep red solution was filtered and left to evaporate at RT. Red hexagonal crystals were collected by filtration after 2 d (0.178 g, 14% based on Mo). $^1$H NMR ($D_2O$): $\delta = 1.25$ (t, 36H), 2.05 (m, 4H), 2.30 (m, 2H), 3.03 (q, 24H), 4.14 (s, 4H), 6.92 (m, 4H), 7.29 ppm (m, 4H); IR (KBr pellets): $\tilde{\nu} = 1506$ (w), 1461 (m), 1389 (w), 1256 (m), 1160 (sh), 1139 (s), 1120 (s), 1045 (vs), 1026 (s), 967 (vs), 945 (sh), 926 (s), 876 (m), 804 (m), 766 (m), 733 cm$^{-1}$ (s); elemental analysis calcd (%) for $C_{46}H_{136}Mo_4N_8O_{42}P_4$: C 27.88, H 6.92, N 5.66, P 6.25, Mo 19.37; found: C 27.93, H 6.57, N 6.22, P 6.16, Mo 17.05.

**Synthesis of $Na_2Rb_6[(Mo^{VI}_3O_8)_4(O_3PC(C_3H_6NH_3)OPO_3)_4]\cdot 26H_2O$ (5)**: $H_4$**Ale** (0.929 g, 3.73 mmol) was added to a solution of $Na_2MoO_4\cdot 2H_2O$ (2.72 g, 11.2 mmol) in water (30 mL). Concentrated hydrochloric acid was added dropwise to pH 3.0. The solution was then stirred for 30 min before addition of solid RbCl (0.9 g, 7.44 mmol). The solution was allowed to stir for another 2 h, during which time a fine white powder slowly precipitated. This solid was filtered off and the filtrate left to evaporate at RT. Colorless crystals were collected the following day (yield 0.429 g, 12% based on Mo). IR (KBr pellets): $\tilde{\nu} = 1505$ (m), 1469 (m), 1452 (m), 1397 (w), 1333 (w), 1169 (s), 1128 (s), 1051 (s), 1026 (vs), 964 (sh), 927 (vs), 884 (vs), 762 (s), 743 (w), 697 (s), 652 (s), 598 (w), 555 cm$^{-1}$ (s); elemental analysis calcd (%) for $C_{16}H_{88}Mo_{12}N_4Na_2O_{86}P_8Rb_6$: C 5.23, H 2.42, N 1.53, P 6.75, Na 1.25, Mo 31.36, Rb 13.97; found: C 5.05, H 1.94, N 1.43, P 6.56, Na 1.75, Mo 32.16, Rb 13.59.

**X-ray crystallography**: Data collection was carried out by using a Siemens SMART three-circle diffractometer for all structures except **4** and **5**, for which data were collected by using a Bruker Nonius X8 APEX 2 diffractometer. Both were equipped with a CCD bidimensional detector using the monochromatized wavelength $\lambda(Mo_{K\alpha}) = 0.71073$ Å. Data were collected at RT for **1**–**3** and **5**, and at 100 K for **4** because these crystals were unstable due to loss of water of hydration. Absorption corrections were based on multiple and symmetry-equivalent reflections in the data set by using the SADABS program,[24] based on the method of Blessing.[25] Structures were solved by direct methods, and refined by full-matrix least-squares methods by using the SHELXTL package.[26] In all structures there is a discrepancy between the formulae determined by elemental analysis and that deduced from the crystallographic atom list because of the difficulty in locating all the disordered water molecules and alkali metal counterions. Disordered water molecules and alkali metal counterions were thus refined with partial occupancy factors and with isotropic thermal parameters. In the structure of **1**, $NH_4^+$ and $H_2O$ could not be distinguished based on the observed electron densities; therefore, all positions were labeled as O and assigned the oxygen atomic diffusion factor. Crystallographic data are given in Table 3.

CCDC 779541 (**1**), 779542 (**2**), 779543 (**3**), 779544 (**4**), and 779545 (**5**) contain the supplementary crystallographic data for this paper. These data can be obtained free of charge from The Cambridge Crystallographic Data Centre via www.ccdc.cam.ac.uk/data_request/cif.

**NMR measurements**: $^{31}$P NMR spectra were recorded in 5 mm tubes with $^1$H decoupling by using a Bruker AC-300 spectrometer operating at 121.5 MHz. $^{31}$P chemical shifts were referenced to the external standard of 85% $H_3PO_4$. For all compounds, ≈20 mg of sample was dissolved in $D_2O$ (700 μL), except for **5**, which was dissolved in 700 μL of a mixture of $D_2O$ (10%) and NaOAc/AcOH buffer (90%, 1 M). The concentrations thus varied between 2–8 mM. For the kinetic study, compound **2** (20 mg, 1.34 $10^{-5}$ mol) was dissolved in LiCl (600 μL, 1 M, pH 3.7) solution to which 100 μL of $D_2O$ was added.

**Infrared spectra**: IR spectra were recorded by using an IRFT Magna 550 Nicolet spectrophotometer on KBr pellets.

**Cell growth inhibition assays**: Human tumor cell lines MCF-7 (breast adenocarcinoma), NCI-H460 (lung large cell), and SF-268 (central nervous system glioblastoma) were obtained from the National Cancer Institute and maintained at 100% humidity and 5% $CO_2$ at 37 °C. Cell lines were cultured in RPMI-1640 medium supplemented with 2 mM L-glutamine and 10% fetal bovine serum (Gibco, Grand Island, NY) at 37 °C in a 5% $CO_2$ atmosphere with 100% humidity. Compound stock solutions were typically prepared in water at a concentration of 0.04 M. A broth microdilution method was used to determine the growth inhibition $IC_{50}$ values of the bisphosphonates. Compounds were half-log serially diluted with cell culture media into 96-well tissue-culture (TC)-treated round-bottom plates (Corning, Corning, NY), typically from 1264 μM to 40 nM, but in

Table 3. Crystallographic data for **1**–**5**.

| | **1** | **2** | **3** | **4** | **5** |
|---|---|---|---|---|---|
| formula | $C_8H_{66}Mo_6N_8O_{44}P_4$ | $C_{24}H_{78}Mo_4N_6O_{28}P_4$ | $C_{16}H_{134}Li_8Mo_8N_4O_{93}P_8$ | $C_{46}H_{136}Mo_4N_8O_{42}P_4$ | $C_{16}H_{88}Mo_{12}N_4Na_2O_{86}P_8Rb_6$ |
| $M_r$ | 1678.18 | 1406.56 | 2942.07 | 1981.26 | 3670.72 |
| crystal system | orthorhombic | triclinic | triclinic | triclinic | monoclinic |
| space group | $P2_12_12$ | $P\bar{1}$ | $P\bar{1}$ | $P\bar{1}$ | $P2_1/c$ |
| $a$ [Å] | 14.274(2) | 9.4664(8) | 17.0185(1) | 13.970(1) | 20.7814(6) |
| $b$ [Å] | 17.412(2) | 11.0739(9) | 17.248(1) | 14.063(1) | 21.2334(6) |
| $c$ [Å] | 9.583(1) | 14.062(1) | 17.610(2) | 20.784(2) | 29.3749(7) |
| $\alpha$ [°] | 90 | 78.103(2) | 96.874(2) | 72.948(4) | 90 |
| $\beta$ [°] | 90 | 72.168(2) | 104.411(2) | 74.989(4) | 134.944(1) |
| $\gamma$ [°] | 90 | 85.285(2) | 94.772(1) | 61.029(4) | 90 |
| $V$ [Å$^3$] | 2381.8(6) | 1372.9(2) | 4936.1(8) | 3381.7(5) | 9174.4(2) |
| $Z$ | 2 | 1 | 2 | 2 | 4 |
| $\rho_{calcd}$ [g cm$^{-3}$] | 2.322 | 1.687 | 1.979 | 1.544 | 2.417 |
| $\mu$ [mm$^{-1}$] | 1.793 | 1.091 | 1.243 | 0.901 | 4.997 |
| data/parameters | 7022/289 | 7750/291 | 27807/1123 | 12086/761 | 16137/1098 |
| $R_{int}$ | 0.0624 | 0.0374 | 0.0298 | 0.0520 | 0.0488 |
| GOF | 1.081 | 0.995 | 1.032 | 1.095 | 1.185 |
| $R$ [$I > 2\sigma(I)$] | $R_1 = 0.0599$, $wR_2 = 0.1340$ | $R_1 = 0.0585$, $wR_2 = 0.1381$ | $R_1 = 0.0519$, $wR_2 = 0.1441$ | $R_1 = 0.0533$, $wR_2 = 0.1561$ | $R_1 = 0.0664$, $wR_2 = 0.1682$ |

  

some cases compounds were run over a larger concentration range to enable accurate $IC_{50}$ determinations. Cells were plated at a density of 5000 cells per well, then incubated under the same culture conditions for 4 d, at which time an MTT ((3-(4,5-dimethylthiazole-2-yl)-2,5-diphenyltetrazolium bromide) cell proliferation assay (ATCC, Manassas, VA) was performed to obtain dose–response curves. Briefly, cells were incubated for 2 h under culture conditions with the tetrazolium salt, lysed with detergent, and incubated overnight, protected from light at RT. The absorbance at $\lambda = 600$ nm was read the following day by using a SpectraMax Plus 384 spectrophotometer (Molecular Devices, Sunnyvale, CA). The compound concentrations for 50% growth inhibition ($IC_{50}$) were obtained by fitting absorbance data to a rectangular hyperbolic function $I = (I_{max})(C)/IC_{50} + C$, in which $I$ is the percentage inhibition, $I_{max} = 100\%$ inhibition, and $C$ is the concentration of the inhibitor, by using GraphPad PRISM 3.0 software for windows (Graphpad Software, San Diego, CA).

## Acknowledgements

This work was supported, in part, by the United States Public Health Service (NIH grants AI074233 and GM65307, to E.O.).

[1] R. G. Russell, Z. Xia, J. E. Dunford, U. Oppermann, A. Kwaasi, P. A. Hulley, K. L. Kavanagh, J. T. Triffitt, M. W. Lundy, R. J. Phipps, B. L. Barnett, F. P. Coxon, M. J. Rogers, N. B. Watts, F. H. Ebetino, *Ann. N. Y. Acad. Sci.* **2007**, *1117*, 209.

[2] Y. Zhang, R. Cao, F. Yin, M. P. Hudock, R. T. Guo, K. Krysiak, S. Mukherjee, Y. G. Gao, H. Robinson, Y. Song, J. H. No, K. Bergan, A. Leon, L. Cass, A. Goddard, T. K. Chang, F. Y. Lin, E. Van Beek, S. Papapoulos, A. H. Wang, T. Kubo, M. Ochi, D. Mukkamala, E. Oldfield, *J. Am. Chem. Soc.* **2009**, *131*, 5153.

[3] M. Coscia, E. Quaglino, M. Iezzi, C. Curcio, F. Pantaleoni, C. Riganti, I. Holen, H. Mönkkönen, M. Boccadoro, G. Forni, P. Musiani, A. Bosia, F. Cavallo, M. Massaia, *J. Cell Mol. Med.* **2009**, DOI: 10.1111/j.1582-4934.2009.00926.x..

[4] M. B. Martin, J. S. Grimley, J. C. Lewis, H. T. Heath III, B. N. Bailey, H. Kendrick, V. Yardley, A. Caldera, R. Lira, J. A. Urbina, S. N. Moreno, R. Docampo, S. L. Croft, E. Oldfield, *J. Med. Chem.* **2001**, *44*, 909.

[5] A. P. Singh, Y. Zhang, J. H. No, R. Docampo, V. Nussenzweig, E. Oldfield, *Antimicrob. Agents Chemother.* **2010**, *54*, 2987.

[6] E. Matczak-Jon, V. Videnova-Adrabińska, *Coord. Chem. Rev.* **2005**, *249*, 2458.

[7] For examples, see the following reviews: a) J. T. Rhule, C. L. Hill, D. A. Judd, R. F. Schinazi, *Chem. Rev.* **1998**, *98*, 327; b) B. Hasenknopf, *Front. Biosci.* **2005**, *10*, 275; c) H. Yanagie, A. Ogata, S. Mitsui, T. Hisa, T. Yamase, M. Eriguchi, *Biomed. Pharmacother.* **2006**, *60*, 349.

[8] Y.-F. Song, N. McMillan, D.-L. Long, S. Kane, J. O. Malm, M. Riehle, C. P. Pradeep, N. Gadegaard, L. Cronin, *J. Am. Chem. Soc.* **2009**, *131*, 1340.

[9] a) M. T. Pope in *Heteropoly and Isopoly Oxometalates*, Springer, New York, **1983**; b) *Polyoxometalates: From Platonic Solids to Anti-Retroviral Activity* (Eds.: M. T. Pope, A. Müller), Kluwer Academic Publishers, : Dordrecht, **1994**.

[10] V. S. Sergienko, *Crystallogr. Rep.* **1999**, *44*, 877, and references therein.

[11] U. Kortz, M. T. Pope, *Inorg. Chem.* **1995**, *34*, 3848.

[12] U. Kortz, M. T. Pope, *Inorg. Chem.* **1995**, *34*, 2160.

[13] H. Tan, W. Chen, D. Liu, Y. Li, E. Wang, *Dalton Trans.* **2010**, *39*, 1245.

[14] a) C. du Peloux, A. Dolbecq, P. Mialane, J. Marrot, F. Sécheresse, *Dalton Trans.* **2004**, 1259; b) A. Dolbecq, L. Lisnard, P. Mialane, J. Marrot, M. Bénard, M.-M. Rohmer, F. Sécheresse, *Inorg. Chem.* **2006**, *45*, 5898; c) A. Dolbecq, J.-D. Compain, P. Mialane, J. Marrot, F. Sécheresse, B. Keita, L. R. Brudna Holze, F. Miserque, L. Nadjo, *Chem. Eur. J.* **2009**, *15*, 733.

[15] a) G. Zhang, B. Keita, A. Dolbecq, P. Mialane, F. Miserque, L. Nadjo, *Chem. Mater.* **2007**, *19*, 5821; b) B. Keita, G. Zhang, A. Dolbecq, P. Mialane, F. Sécheresse, F. Miserque, L. Nadjo, *J. Phys. Chem. A* **2007**, *111*, 8145.

[16] J.-D. Compain, A. Dolbecq, J. Marrot, P. Mialane, F. Sécheresse, *C. R. Chim.* **2010**, *13*, 329.

[17] I. Shinkai, Y. Ohta, *Res. Prog. Org.-Biol. Med. Chem.* **1996**, *4*, 3, and references therein.

[18] N. E. Brese, M. O'Keeffe, *Acta Crystallogr. Sect. B* **1991**, *47*, 192.

[19] a) Q. Chen, J. Zubieta, *Coord. Chem. Rev.* **1992**, *114*, 107; b) H. K. Chae, W. G. Klemperer, T. A. Macquart, *Coord. Chem. Rev.* **1993**, *128*, 209; c) B. Modec, J. V. Brenčič, *J. Cluster Sci.* **2002**, *13*, 279.

[20] J.-D. Compain, P. Deniard, R. Dessapt, A. Dolbecq, O. Oms, F. Sécheresse, J. Marrot, P. Mialane, unpublished results.

[21] For example, see: a) C. Boglio, G. Lenoble, C. Duhayon, B. Hasenknopf, R. Thouvenot, C. Zhang, R. C. Howell, B. P. Burton-Pye, L. C. Francesconi, E. Lacôte, S. Thorimbert, M. Malacria, C. Afonso, J.-C. Tabet, *Inorg. Chem.* **2006**, *45*, 1389; b) M. Kozik, L. C. W. Baker, *J. Am. Chem. Soc.* **1990**, *112*, 7604; c) P. Mialane, A. Dolbecq, L. Lisnard, A. Mallard, J. Marrot, F. Sécheresse, *Angew. Chem.* **2002**, *114*, 2504; *Angew. Chem. Int. Ed.* **2002**, *41*, 2398.

[22] L. Lisnard, P. Mialane, A. Dolbecq, J. Marrot, F. Sécheresse, *Inorg. Chem. Commun.* **2003**, *6*, 503.

[23] V. Kubíček, J. Kotek, P. Hermann, I. Lukeš, *Eur. J. Inorg. Chem.* **2007**, 333.

[24] SADABS, program for scaling and correction of area detector data, G. M. Sheldrick, University of Göttingen (Germany), **1997**.

[25] R. Blessing, *Acta Crystallogr. Sect. A* **1995**, *51*, 33.

[26] SHELX-TL version 5.03, Software Package for Crystal Structure Determination, G. M. Sheldrick, Siemens Analytical X-ray Instrument Division, Madison, **1994**.

Received: June 9, 2010
Published online: October 18, 2010

  